

Optimized trajectory unraveling for classical simulation of noisy quantum dynamics

Zhuo Chen,^{1,2} Yimu Bao,³ and Soonwon Choi¹

¹*Center for Theoretical Physics, Massachusetts Institute of Technology, Cambridge, MA 02139, USA*

²*The NSF AI Institute for Artificial Intelligence and Fundamental Interactions, Cambridge, MA 02139, USA*

³*Department of Physics, University of California, Berkeley, California 94720, USA*

The dynamics of open quantum systems can be simulated by unraveling it into an ensemble of pure state trajectories undergoing non-unitary monitored evolution, which has recently been shown to undergo measurement-induced entanglement phase transition. Here, we show that, for an arbitrary decoherence channel, one can optimize the unraveling scheme to lower the threshold for entanglement phase transition, thereby enabling efficient classical simulation of the open dynamics for a broader range of decoherence rates. Taking noisy random unitary circuits as a paradigmatic example, we analytically derive the optimum unraveling basis that on average minimizes the threshold. Moreover, we present a heuristic algorithm that adaptively optimizes the unraveling basis for given noise channels, also significantly extending the simulatable regime. When applied to noisy Hamiltonian dynamics, the heuristic approach indeed extends the regime of efficient classical simulation based on matrix product states beyond conventional quantum trajectory methods. Finally, we assess the possibility of using a quasi-local unraveling, which involves multiple qubits and time steps, to efficiently simulate open systems with an arbitrarily small but finite decoherence rate.

Introduction.— While an ideal quantum system evolves under unitary evolution according to the Schrödinger’s equation, realistic quantum systems are inevitably subject to environmental noise and undergo open system dynamics, often well modeled by the Lindblad equation [1]. Efficient classical simulation of such dynamics not only enables theoretical understanding of open quantum systems but is also pivotal in advancing quantum simulation experiments [2–4] and benchmarking near-term quantum devices [5, 6].

Stochastic wavefunction method is a widely-adopted approach to simulate open system dynamics [7–11]. In this method, instead of simulating the evolution of the mixed density matrix describing the open system, one *unravels* the mixed state into an ensemble of pure quantum trajectories whose statistical average emulates the evolution of the mixed state. Interestingly, each trajectory in the ensemble follows non-unitary evolution that can be understood as monitored quantum dynamics, wherein entanglement can undergo a measurement-induced phase transition from a volume- to an area-law scaling when the noise or decoherence rate increases [12–17]. Since the simulation cost grows exponentially with entanglement entropy and, in particular, the area-law scaling of entanglement implies efficient representation of quantum states in one dimension using matrix product states (MPS) [18–21], this phenomenon indicates the presence of a critical decoherence rate above which efficient classical simulation is feasible in one dimension.

Importantly, the same open system dynamics can be unraveled into infinitely many equivalent trajectory ensembles, and the entanglement entropy within trajectories strongly depends on the unraveling scheme. In a pioneering work, Ref. [22] focused on two classes of unraveling schemes and designed an entanglement-optimized algorithm that minimizes the entanglement growth at

each time step. Independently, Ref. [23] considered random unitary circuits (RUC) with dephasing noise and focused on four empirically chosen unraveling schemes, and found that two of them result in a lower critical decoherence rate compared to the conventional unraveling using projective measurements. Yet, it remains open, for generic quantum evolution subject to a generic type of decoherence, whether one can systematically obtain an unraveling scheme that minimizes the critical decoherence rate and extends the regime of efficient simulation.

In this paper, we show that, for arbitrary types of decoherence, one can obtain an unraveling scheme that optimizes the critical decoherence rate and therefore extends the regime of efficient classical simulation. We consider the most general form of unraveling schemes that involve a minimum number of Kraus operators for each decoherence channel. As a paradigmatic example, we first focus on noisy random unitary circuits [Fig. 1(a)] and obtain an analytic expression for an optimized unraveling basis that minimizes the critical threshold on average based on an effective spin model. Subsequently, we propose a heuristic algorithm that adaptively optimizes the unraveling basis for a given arbitrary quantum channel to maximally disentangle individual noisy qubits from the rest in each simulation step. Both methods significantly extend the regime of classical simulation. We then apply our heuristic algorithm to simulate noisy Hamiltonian dynamics and demonstrate how classical simulation, utilizing MPS, becomes viable for low decoherence rates that were previously not feasible. We further discuss the possibility to extend the efficient simulation regime to any small but finite decoherence rate based on a quasi-local unraveling scheme, where multiple qubits and time steps are jointly unraveled [Fig. 1(c)].

We note that alternative methods for simulating noisy evolution have been proposed based on matrix prod-

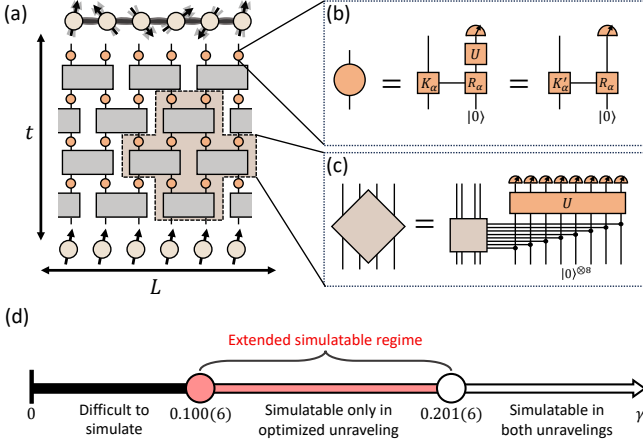


FIG. 1. (a) Quantum evolution subject to generic local decoherence. The time evolution is digitized into a quantum circuit with local decoherence channels. (b) The decoherence channel can be expressed as a coupling to an ancilla qudit and measuring the ancilla qudit, where the coupling gate is determined by the Kraus operators K_α and a rotation gate on the ancilla qudit $R_\alpha = \sum_{\beta=0}^{N-1} |\alpha + \beta \bmod N\rangle\langle\beta|$. Equivalent unravelings can differ by a unitary gate U on the ancilla qudit, which results in an equivalent set of Kraus operators $K'_\alpha = \sum_\beta U_{\alpha\beta} K_\beta$. (c) Multiple unitary gates and decoherence channels can be combined into a two-qudit quantum channel, which can be purified by applying a joint unitary gate on the ancilla and system qudits. (d) Phase diagram for simulating mixed-field Ising model with dephasing noise using trajectory unraveling. The unraveling in computational basis yields a critical error rate of $\gamma_c = 0.201(6)$, whereas the optimized unraveling reduces the critical rate down to $\gamma_c = 0.100(6)$.

uct representation of the density matrix [24–27]. However, these methods suffer from issues such as failure to maintain the positivity of the density matrix and lack of controlled approximation for the evolution. Besides, Ref. [28] showed the existence of an efficient classical algorithm for noisy random circuits with any finite decoherence rate, but the algorithm is difficult to implement in practice.

Unraveling open system dynamics.— The dynamics of a one-dimensional system in a Markovian noisy environment is generally described by the Lindblad equation [1]. Here, we consider a discretized evolution, in which the dissipative part of the Lindblad equation acts on the system as quantum channels [29] [see Fig. 1(a)]. We focus on the unraveling of these quantum channels that decohere the underlying unitary evolution.

A generic quantum channel can be always decomposed in terms of the Kraus operators K_α

$$\mathcal{N}[\rho] = \sum_{\alpha=0}^{N-1} K_\alpha \rho K_\alpha^\dagger, \quad (1)$$

where K_α satisfies $\sum_{\alpha=0}^{N-1} K_\alpha^\dagger K_\alpha = \mathbb{1}$. Such a decoher-

ence channel can be formulated as unitary coupling U_{QM} between the system Q and an ancilla qudit M ; tracing out the ancilla qudit reproduces the quantum channel [30], i.e.

$$\mathcal{N}[\rho] = \text{tr}_M \left(U_{QM} (\rho \otimes |0\rangle\langle 0|) U_{QM}^\dagger \right), \quad (2)$$

where $U_{QM} = \sum_{\alpha,\beta=0}^{N-1} K_\alpha \otimes |\alpha + \beta \bmod N\rangle\langle\beta|$, and the ancilla qudit is of dimension N same as the number of Kraus operators.

Tracing the ancilla qudit is equivalent to summing over an ensemble of trajectories generated by measuring the ancilla qudit in a computational basis. The probability of the measurement outcome α is determined by the Born rule. In each trajectory associated with the outcome α , a Kraus operator K_α acts on the system. Such an ensemble of trajectories averages to the mixed density matrix $\mathcal{N}[\rho]$ and therefore serves as an unraveling of the channel.

Crucially, the quantum channel can be unraveled in infinitely many equivalent ways. Equivalent schemes can be obtained by measuring the ancilla qudit in a rotated basis and thus are related by a unitary transformation U as in Fig. 1(b) [31]. Alternatively, the unitary rotation U on the ancilla qudit can be viewed as decomposing \mathcal{N} in terms of a different set of Kraus operators related to $\{K_\alpha\}$ by $K'_\alpha = \sum_\beta U_{\alpha\beta} K_\beta$. In the rest of the paper, we take either perspective on relating equivalent unraveling schemes, whichever is convenient.

The challenge for efficient classical simulation lies in the entanglement entropy within each trajectory. To illustrate this, we consider the evolution subject to local dephasing noise of rate p , described by $\mathcal{N}_{\phi,i}[\rho] = (1 - p/2)\rho + (p/2)Z_i\rho Z_i$. The channel can be unraveled into probabilistic projective measurement in the Pauli-Z basis with probability p . It has been shown that such a unitary evolution interspersed by measurements exhibits a measurement-induced transition in the half-chain entanglement entropy from a volume- to an area-law scaling [12–14]. This indicates the classical simulation of trajectory dynamics is efficient only above the critical decoherence rate p_c .

However, p_c depends on the unraveling basis. For example, the dephasing channel $\mathcal{N}_{\phi,i}$ can be also unraveled into trajectories in which a Z_i gate is applied with probability $p/2$. In this unraveling, every trajectory undergoes purely unitary evolution and is generally always in the volume-law phase, making it difficult to simulate classically. Our goal is to find an optimized unraveling basis that minimizes p_c and extends the regime of efficient simulation.

Optimized unraveling for noisy random unitary circuits.— We first consider the trajectory unraveling of noisy random unitary circuits (RUC) operating on a one-dimensional chain of qudits with local Hilbert space dimension q . The circuit involves two-qudit Haar random unitary gates arranged in a brick-layer structure and lo-

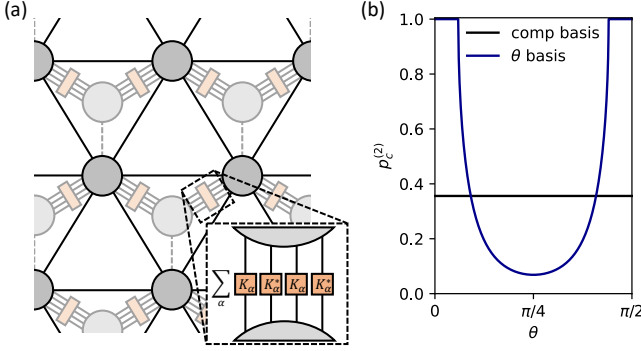


FIG. 2. (a) Effective Ising spin model on a triangular lattice for noisy random unitary circuits (RUC). The Ising couplings between spins on the same downward-facing triangle depend on the unraveling scheme, i.e. the Kraus operators K_α . (b) Critical point $p_c^{(2)}$ in the spin model for various unraveling schemes of the RUC with dephasing noise. The black and blue lines represent $p_c^{(2)}$ in the conventional unraveling based on projective measurements, and general unraveling schemes involving two Kraus operators, respectively. $p_c^{(2)}$ in the general unraveling scheme as a function of θ for fixed $\phi = \pi/4$ is presented. The lowest $p_c^{(2)}$ is obtained at $\theta = \phi = \pi/4$.

cal decoherence channels applied to every single qudit after each layer as shown in Fig. 1(a).

The entanglement entropy in the trajectories of noisy Haar random circuits has an analytic albeit approximate description in terms of the domain wall free energy in a two-dimensional classical Ising spin model on a triangular lattice [Fig. 2 (a)] [32, 33]. The spin model exhibits a ferromagnetic transition when tuning the decoherence rate, which is detected by the domain wall free energy and corresponds to the transition in the entanglement entropy. The couplings in the spin model are between the neighboring spins in the triangular lattice and depend on both the decoherence rate and unraveling scheme. Remarkably, in the case that every channel is unraveled in the same basis, the spin model is translationally invariant, and its critical point $p_c^{(2)}$ is exactly solvable [34, 35]. Thus, we can determine an optimized unraveling basis for the RUC that exactly minimizes the analytically determined critical decoherence rate $p_c^{(2)}$. We note that the spin model only describes the quasi-entropy, and its critical point $p_c^{(2)}$ approximates p_c in the true von Neumann entropy. Yet, the unraveling basis that minimizes $p_c^{(2)}$ still greatly reduces the p_c for von Neumann entropy, which will be numerically demonstrated in Fig. 3.

Specifically, for a given unraveling scheme, i.e. a set of Kraus operators $\{K_\alpha\}$ depending on the decoherence rate p , the critical point $p_c^{(2)}$ in the spin model can be determined from [32]

$$\left(\frac{u_2}{u_1}\right)^2 - 2\frac{q^2 - 1}{q^2 + 1} \left(\frac{u_2}{u_1}\right) - 1 = 0, \quad (3)$$

where

$$u_2 = \sum_{\alpha=0}^{N-1} (\text{tr } K_\alpha^\dagger K_\alpha)^2, \quad u_1 = \sum_{\alpha=0}^{N-1} \text{tr } K_\alpha^\dagger K_\alpha K_\alpha^\dagger K_\alpha. \quad (4)$$

We optimize the critical threshold $p_c^{(2)}$ in the spin model over equivalent sets of Kraus operators related by unitary transformations U . For the dephasing channel, it turns out $p_c^{(2)}$ depends on two parameters θ and ϕ [29], and the optimum is found at $\theta = \phi = \pi/4$ with $p_c^{(2)} = 0.0685$, which is significantly lower than $p_c^{(2)} = 0.3558$ in the conventional unraveling based on projective measurements [32]. The resulting Kraus operators are $K_{0,1} = (\pm\sqrt{1-p/2}1 + \sqrt{p/2}Z)/\sqrt{2}$, which coincides with those in one unraveling scheme studied in Ref. [23] up to a sign difference. Our method can be applied to an arbitrary type of decoherence channel. For depolarization and amplitude damping noise, we obtain the spin-model optimized basis with corresponding $p_c^{(2)}$ in the Supplementary Material [29].

So far, we only consider optimizing the critical decoherence rate $p_c^{(2)}$ in the spin model. However, the entanglement within the simulatable regime, i.e. the area-law phase, may not be optimally minimized. With this analytic tool, it is worth exploring whether one can minimize the quasi-entropy within the area-law phase to further reduce the computational cost of classical simulation.

Exactly solving the spin model can determine an unraveling basis that is optimized on average for all random circuit realizations and trajectories. However, in practice, the optimal basis for each decoherence channel depends on the specific quantum state it applies to and therefore can vary among different trajectories. Here, we propose a heuristic algorithm that optimizes the unraveling for each individual decoherence channel. The most straightforward idea is to find the unraveling basis that results in the minimum entanglement in the system. However, such an optimization process is computationally expensive, and we instead search for the basis that maximally and locally disentangles the noisy qubit from the rest of the system. Specifically, we first compute the reduced density matrix ρ_i of the noisy qubit. Then, we optimize over equivalent Kraus decompositions of the decoherence channel such that the average entanglement between the noisy qubit and the rest is minimized.

To demonstrate the optimized unraveling schemes indeed lowers p_c , we perform an exact numerical simulation of Haar random unitary circuits subject to dephasing noise operating on a chain of qubits ($q = 2$) up to system size $L = 24$ with periodic boundary condition. We compute the tripartite mutual information $I_3 = S_A + S_B + S_C - S_{AB} - S_{AC} - S_{BC} + S_{ABC}$ to determine the critical point p_c , where A , B , and C each represents a quarter of the system. Such a quantity is expected to change sharply from a volume-law scaling

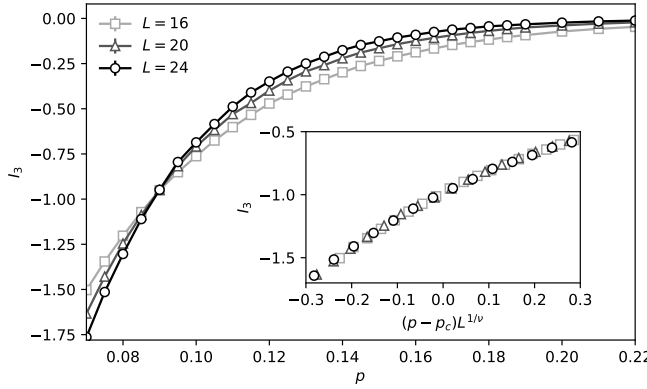


FIG. 3. Tripartite mutual information I_3 as a function of the decoherence rate p in the spin-model optimized unraveling for RUC. The results are obtained from exact simulation up to system size $L = 24$. (Inset) Finite-size scaling collapse determines the critical decoherence rate $p_c = 0.089(3)$. For comparisons, conventional unraveling based on projective measurements in computational basis yields $p_c = 0.168(3)$, and the heuristically optimized unraveling basis $p_c = 0.085(2)$. The results are averaged over 400 quantum trajectories.

$I_3 = \mathcal{O}(L)$ to an area-law scaling $I_3 = \mathcal{O}(1)$ across the phase transition [36]. In Fig. 3, we perform the finite-size scaling using the ansatz $I_3 = \mathcal{F}((p - p_c)L^{1/\nu})$ to extract p_c . Compared to the conventional unraveling based on projective measurements with $p_c = 0.168(3)$ [29, 36], the optimized unravelings obtained from the spin model and from the heuristic algorithm yield significantly lower critical decoherence rates $p_c = 0.089(3)$ and $p_c = 0.085(2)$, respectively.

Optimized unraveling for Hamiltonian dynamics with dephasing noise.— The optimized unraveling scheme can also extend the regime of efficient simulation for noisy Hamiltonian dynamics. Here, we study the one-dimensional mixed-field Ising model (MFIM) under dephasing noise, which is governed by the Lindblad equation $\dot{\rho} = -i[H, \rho] + \gamma \sum_i (Z_i \rho Z_i^\dagger - \frac{1}{2} \{Z_i^\dagger Z_i, \rho\})$. We consider $H = -\sum_{\langle i,j \rangle} Z_i Z_j + 1.05 \sum_i X_i - 0.5 \sum_i Z_i$, which is far from any integrable system and is challenging to simulate in the absence of decoherence [37]. We remark that the trotterized evolution of the Lindblad equation can be represented in the brick-layer structure in Fig. 1(a), where the quantum channels are $\mathcal{N}_{\phi,i}$ of dephasing rate $p = 2\gamma dt$.

We first apply our heuristic algorithm to exactly simulate the noisy dynamics. The finite size scaling analysis yields the critical decoherence rate $\gamma_c = 0.100(6)$, which is significantly lower than $\gamma_c = 0.201(6)$ obtained in the conventional unraveling [29].

The optimized unraveling allows simulating the noisy dynamics of an arbitrarily large system based on MPS in an extended regime. In the MPS simulation, the required bond dimension χ grows exponentially with the system size [$\chi \sim \mathcal{O}(\exp(L))$] in the volume-law phase,

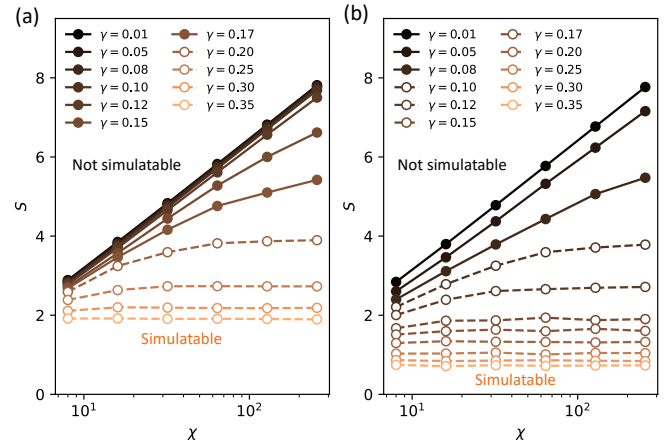


FIG. 4. Half-chain entanglement entropy S in the steady state as a function of bond dimension χ in MPS simulation for MFIM with dephasing noise. We consider the system size $L = 100$ and compare the entanglement in (a) unraveling in the computational basis and (b) optimized unraveling for various dephasing rates γ . Dashed lines with empty circles and solid lines with filled circles represent data points in the area- and volume-law phases, respectively.

while the required χ is only a constant [$\chi \sim \mathcal{O}(1)$] in the area-law phase. We use two unraveling schemes to simulate the noisy MFIM of system size $L = 100$, where the exact simulation is not possible. Indeed, we find that, for a relatively small bond dimension $\chi \leq 256$, the entanglement saturates, and the MPS can capture the trajectory dynamics for $\gamma \geq 0.2$ in the conventional unraveling scheme, whereas the entanglement saturates in an extended regime $\gamma \geq 0.1$ in the optimized basis (Fig. 4).

Discussion.— We have introduced optimized unraveling schemes for trajectory simulation of one-dimensional open system dynamics under arbitrary types of decoherence. We focused on the single-qubit unraveling and showed that the classical simulation is efficient when the decoherence rate is above a significantly reduced but finite p_c (γ_c). These results open multiple directions for future research.

By unraveling multiple noisy channels at the same time, an efficient simulation may be possible for noisy dynamics with any non-vanishing decoherence rate γ . The entanglement between the system and ancilla qudits is generated at the rate of γ . Over a time period $T \gtrsim 1/\gamma$, each system qudit becomes decohered and only entangles with the ancilla qudits. Thus, considering an optimized unraveling basis over LT ancilla qudits for all noisy channels within this period, one can disentangle the system in each trajectory into a short-range entangled state [38]. However, this procedure generally requires optimization over a nonlocal unitary rotation on LT ancilla qudits, which is computationally challenging. It remains open whether one can find an efficient representation of the optimized unraveling basis over LT ancilla qudits.

Alternatively, one can take a coarse-grained perspective on noisy random circuits. Specifically, we combine all the gates and decoherence channels within a diamond-shaped region into a single quantum channel on two qudits, each involving m consecutive qubits in the original circuit [as shown Fig. 1 (a,c)]. Although each diamond-shaped block contains $\mathcal{O}(m^2)$ two-qubit unitary gates, only $\mathcal{O}(m)$ gates support on both qudits and generate entanglement between them. In contrast, decoherence within each block generates $\mathcal{O}(m^2)$ entanglement between the system and ancilla qudits. Thus, after the coarse-graining, the effective decoherence rate increases by m ; we expect a reduced critical decoherence rate $\gamma_c = \mathcal{O}(1/m)$ if we optimize the unraveling basis over the coarse-grained noisy channel. Hence, by grouping $m \sim 1/\gamma$ qubits in a single qudit and obtaining the optimized unraveling for noisy channels acting on two qudits, one can facilitate efficient simulation at an arbitrarily small but finite γ . We leave for future work to develop an explicit algorithm to realize this idea. We remark that such an algorithm only involves finding optimized unraveling for polynomially many decoherence channels that involve $\mathcal{O}(m^2)$ ancilla qudits, which is at a cost of $\mathcal{O}(\exp(m^2)) \sim \mathcal{O}(\exp(1/\gamma^2))$. The polynomial resource in system size L is consistent with previous results from both theoretical complexity analysis [28] and numerical simulation based on matrix product operators [26].

Another future direction is to study the optimized unraveling for open system dynamics in higher dimensions. In this case, bipartite entanglement does not on its own determine the cost of classical simulation. It remains open how to design an unraveling scheme to reduce the complexity of simulating trajectory dynamics on classical computers.

Furthermore, it is of great practical interest to simulate noisy evolution in near-term quantum simulation platforms based on the optimized trajectory unraveling. On one hand, the classical simulation allows benchmarking near-term devices [5, 39]. On the other hand, the input from classical simulation combined with samples from quantum simulators may allow probing “computationally assisted” observables [40–42] that are difficult to compute by classical computers alone.

Acknowledgement.— The authors acknowledge Hannes Pichler and Tianci Zhou for insightful discussions, and Matteo Ippoliti for helpful feedback on the manuscript.

Note added: Upon completion of the present manuscript, we became aware of an independent work on related topics appearing on arXiv on the same day [43]. Our works are complementary, and our results agree where they overlap.

- [1] H.-P. Breuer, F. Petruccione, *et al.*, *The theory of open quantum systems* (Oxford University Press on Demand, 2002).
- [2] F. Arute, K. Arya, R. Babbush, D. Bacon, J. C. Bardin, R. Barends, R. Biswas, S. Boixo, F. G. Brandao, D. A. Buell, *et al.*, Quantum supremacy using a programmable superconducting processor, *Nature* **574**, 505 (2019).
- [3] Y. Wu, W.-S. Bao, S. Cao, F. Chen, M.-C. Chen, X. Chen, T.-H. Chung, H. Deng, Y. Du, D. Fan, *et al.*, Strong quantum computational advantage using a superconducting quantum processor, *Physical Review Letters* **127** (2021).
- [4] R. Acharya, I. Aleiner, R. Allen, T. I. Andersen, M. Ansmann, F. Arute, K. Arya, A. Asfaw, J. Atalaya, R. Babbush, *et al.*, Suppressing quantum errors by scaling a surface code logical qubit, *Nature* **614**, 676 (2023).
- [5] J. Choi, A. L. Shaw, I. S. Madjarov, X. Xie, R. Finkelstein, J. P. Covey, J. S. Cotler, D. K. Mark, H.-Y. Huang, A. Kale, *et al.*, Preparing random states and benchmarking with many-body quantum chaos, *Nature* **613**, 468 (2023).
- [6] J. S. Cotler, D. K. Mark, H.-Y. Huang, F. Hernandez, J. Choi, A. L. Shaw, M. Endres, and S. Choi, Emergent quantum state designs from individual many-body wave functions, *PRX Quantum* **4**, 010311 (2023).
- [7] R. Dum, P. Zoller, and H. Ritsch, Monte carlo simulation of the atomic master equation for spontaneous emission, *Physical Review A* **45**, 4879 (1992).
- [8] J. Dalibard, Y. Castin, and K. Mølmer, Wave-function approach to dissipative processes in quantum optics, *Physical Review Letters* **68**, 580 (1992).
- [9] C. W. Gardiner, A. S. Parkins, and P. Zoller, Wave-function quantum stochastic differential equations and quantum-jump simulation methods, *Physical Review A* **46**, 4363 (1992).
- [10] M. B. Plenio and P. L. Knight, The quantum-jump approach to dissipative dynamics in quantum optics, *Reviews of Modern Physics* **70**, 101 (1998).
- [11] H. Carmichael, *An open systems approach to quantum optics: lectures presented at the Université Libre de Bruxelles, October 28 to November 4, 1991*, Vol. 18 (Springer Science & Business Media, 2009).
- [12] Y. Li, X. Chen, and M. P. Fisher, Quantum zeno effect and the many-body entanglement transition, *Physical Review B* **98**, 205136 (2018).
- [13] B. Skinner, J. Ruhman, and A. Nahum, Measurement-induced phase transitions in the dynamics of entanglement, *Physical Review X* **9**, 031009 (2019).
- [14] Y. Li, X. Chen, and M. P. Fisher, Measurement-driven entanglement transition in hybrid quantum circuits, *Physical Review B* **100**, 134306 (2019).
- [15] S. Choi, Y. Bao, X.-L. Qi, and E. Altman, Quantum error correction in scrambling dynamics and measurement-induced phase transition, *Physical Review Letters* **125**, 030505 (2020).
- [16] M. Szyniszewski, A. Romito, and H. Schomerus, Entanglement transition from variable-strength weak measurements, *Physical Review B* **100**, 064204 (2019).
- [17] M. J. Gullans and D. A. Huse, Dynamical purification phase transition induced by quantum measurements, *Physical Review X* **10**, 041020 (2020).

- [18] S. R. White, Density matrix formulation for quantum renormalization groups, *Physical Review Letters* **69**, 2863 (1992).
- [19] G. Vidal, Efficient classical simulation of slightly entangled quantum computations, *Physical Review Letters* **91**, 147902 (2003).
- [20] G. Vidal, Efficient simulation of one-dimensional quantum many-body systems, *Physical Review Letters* **93**, 040502 (2004).
- [21] U. Schollwöck, The density-matrix renormalization group in the age of matrix product states, *Annals of Physics* **326**, 96 (2011), january 2011 Special Issue.
- [22] T. Vovk and H. Pichler, Entanglement-optimal trajectories of many-body quantum markov processes, *Physical Review Letters* **128**, 243601 (2022).
- [23] M. Kolodrubetz, Optimality of lindblad unfolding in measurement phase transitions, *Physical Review B* **107**, L140301 (2023).
- [24] F. Verstraete, J. J. Garcia-Ripoll, and J. I. Cirac, Matrix product density operators: Simulation of finite-temperature and dissipative systems, *Physical Review Letters* **93**, 207204 (2004).
- [25] M. Zwolak and G. Vidal, Mixed-state dynamics in one-dimensional quantum lattice systems: a time-dependent superoperator renormalization algorithm, *Physical Review Letters* **93**, 207205 (2004).
- [26] K. Noh, L. Jiang, and B. Fefferman, Efficient classical simulation of noisy random quantum circuits in one dimension, *Quantum* **4**, 318 (2020).
- [27] C. D. White, M. Zaletel, R. S. Mong, and G. Refael, Quantum dynamics of thermalizing systems, *Physical Review B* **97**, 035127 (2018).
- [28] D. Aharonov, X. Gao, Z. Landau, Y. Liu, and U. Vazirani, A polynomial-time classical algorithm for noisy random circuit sampling, *arXiv preprint arXiv:2211.03999* (2022).
- [29] See supplementary online material for details.
- [30] J. Preskill, Lecture notes for physics 229: Quantum information and computation, California Institute of Technology **16**, 1 (1998).
- [31] In general, U can be isometry. For simplicity, we only optimize over unitary transformations on the ancilla qudit.
- [32] Y. Bao, S. Choi, and E. Altman, Theory of the phase transition in random unitary circuits with measurements, *Physical Review B* **101**, 104301 (2020).
- [33] C.-M. Jian, Y.-Z. You, R. Vasseur, and A. W. Ludwig, Measurement-induced criticality in random quantum circuits, *Physical Review B* **101**, 104302 (2020).
- [34] T. Eggarter, Triangular antiferromagnetic ising model, *Physical Review B* **12**, 1933 (1975).
- [35] Y. Tanaka and N. Uryû, Triangular ising lattice with anisotropic interactions, *Journal of the Physical Society of Japan* **44**, 1091 (1978).
- [36] A. Zabalo, M. J. Gullans, J. H. Wilson, S. Gopalakrishnan, D. A. Huse, and J. Pixley, Critical properties of the measurement-induced transition in random quantum circuits, *Physical Review B* **101**, 060301 (2020).
- [37] M. C. Bañuls, J. I. Cirac, and M. B. Hastings, Strong and weak thermalization of infinite nonintegrable quantum systems, *Physical review letters* **106**, 050405 (2011).
- [38] B. Schumacher and M. D. Westmoreland, Approximate quantum error correction, *Quantum Information Processing* **1**, 5 (2002).
- [39] D. K. Mark, J. Choi, A. L. Shaw, M. Endres, and S. Choi, Benchmarking quantum simulators using quantum chaos, *arXiv preprint arXiv:2205.12211* (2022).
- [40] J. Y. Lee, W. Ji, Z. Bi, and M. Fisher, Decoding measurement-prepared quantum phases and transitions: from ising model to gauge theory, and beyond, *arXiv preprint arXiv:2208.11699* (2022).
- [41] M. J. Gullans and D. A. Huse, Scalable probes of measurement-induced criticality, *Physical Review Letters* **125**, 070606 (2020).
- [42] S. J. Garratt, Z. Weinstein, and E. Altman, Measurements conspire nonlocally to restructure critical quantum states, *Physical Review X* **13**, 021026 (2023).
- [43] Z. Cheng and M. Ippoliti, Efficient sampling of noisy shallow circuits via monitored unraveling, to appear.

Supplementary Online Material for “Optimized trajectory unraveling for classical simulation of noisy quantum dynamics”

Zhuo Chen,^{1,2} Yimu Bao,³ and Soonwon Choi¹

¹*Center for Theoretical Physics, Massachusetts Institute of Technology, Cambridge, MA 02139, USA*

²*The NSF AI Institute for Artificial Intelligence and Fundamental Interactions, Cambridge, MA 02139, USA*

³*Department of Physics, University of California, Berkeley, California 94720, USA*

(Dated: June 30, 2023)

CONTENTS

SI. Unraveling of quantum channels	S1
1. Dephasing channel	S1
2. Amplitude damping channel	S2
3. Depolarization channel	S2
SII. Optimized unraveling based on the effective spin model	S2
1. Dephasing channel	S4
2. Amplitude damping channel	S4
SIII. Details for heuristic optimization algorithm	S5
SIV. Trotterization of Lindblad equation	S5
SV. Additional numerical results	S5
References	S9

SI. UNRAVELING OF QUANTUM CHANNELS

General quantum channel \mathcal{N} can be decomposed into a set of N Kraus operators, i.e.

$$\mathcal{N}[\rho] = \sum_{\alpha=0}^{N-1} K_{\alpha} \rho K_{\alpha}^{\dagger}, \quad (\text{S1})$$

where K_{α} satisfies $\sum_{\alpha} K_{\alpha}^{\dagger} K_{\alpha} = \mathbb{1}$. In this work, we study three decoherence channels in qubit systems—dephasing, amplitude damping, and depolarization channels—as examples to demonstrate our optimized unraveling.

1. Dephasing channel

The dephasing channel in a qubit system is defined as

$$\mathcal{N}_{\phi}[\rho] = \left(1 - \frac{p}{2}\right) \rho + \frac{p}{2} Z \rho Z, \quad (\text{S2})$$

where Z is the Pauli-Z operator.

The conventional unraveling of the dephasing channel is based on projective measurements in a computational basis and can be represented using the following Kraus operators

$$K_0 = \sqrt{1-p} \mathbb{1}, \quad K_1 = \sqrt{p} |0\rangle\langle 0|, \quad K_2 = \sqrt{p} |1\rangle\langle 1|. \quad (\text{S3})$$

Alternatively, the dephasing channel can be unraveled with a minimum number of two Kraus operators

$$K_0 = \sqrt{1 - \frac{p}{2}} \mathbb{1}, \quad K_1 = \sqrt{\frac{p}{2}} Z. \quad (\text{S4})$$

In this unraveling, each Kraus operator is proportional to a unitary operator, and it has the interpretation of applying a Z gate with probability $p/2$. We search for an optimized unraveling scheme related to this minimum set by a unitary transformation

2. Amplitude damping channel

Another example we consider is the amplitude damping channel

$$\mathcal{N}_d \begin{bmatrix} \rho_{00} & \rho_{01} \\ \rho_{10} & \rho_{11} \end{bmatrix} = \begin{pmatrix} \rho_{00} + p\rho_{11} & \sqrt{1-p}\rho_{01} \\ \sqrt{1-p}\rho_{10} & (1-p)\rho_{11} \end{pmatrix} \quad (\text{S5})$$

where p is the damping rate. The channel describes spontaneous decay from $|1\rangle$ to $|0\rangle$ with a probability p .

Conventionally, the channel is written in terms of two Kraus operators

$$K_0 = |0\rangle\langle 0| + \sqrt{1-p}|1\rangle\langle 1|, \quad K_1 = \sqrt{p}|0\rangle\langle 1|. \quad (\text{S6})$$

Here, we consider equivalent unraveling schemes that are related to the conventional unraveling by a unitary transformation.

3. Depolarization channel

The third example we consider is the depolarization channel that describes qubit loss at a probability p

$$\mathcal{N}_p[\rho] = \left(1 - \frac{3p}{4}\right)\rho + \frac{p}{4}X\rho X + \frac{p}{4}Y\rho Y + \frac{p}{4}Z\rho Z. \quad (\text{S7})$$

Conventionally, the depolarization channel is decomposed in terms of the Kraus operators

$$K_0 = \sqrt{1-p}\mathbb{1} \quad K_1 = \sqrt{\frac{p}{2}}|0\rangle\langle 0|, \quad K_2 = \sqrt{\frac{p}{2}}|0\rangle\langle 1|, \quad K_3 = \sqrt{\frac{p}{2}}|1\rangle\langle 0|, \quad K_4 = \sqrt{\frac{p}{2}}|1\rangle\langle 1|, \quad (\text{S8})$$

which corresponds to replacing the noisy qubit with a fresh qubit, randomly sampled from $\{|0\rangle, |1\rangle\}$, with probability p . Alternatively, a minimum number of four Kraus operators is sufficient to describe the same depolarization channel, which reads

$$K_0 = \sqrt{1 - \frac{3p}{4}}\mathbb{1}, \quad K_1 = \sqrt{\frac{p}{4}}X, \quad K_2 = \sqrt{\frac{p}{4}}Y, \quad K_3 = \sqrt{\frac{p}{4}}Z. \quad (\text{S9})$$

Similar to the dephasing channel, the optimal unraveling is parameterized as a unitary transformation from this minimum set.

SII. OPTIMIZED UNRAVELING BASED ON THE EFFECTIVE SPIN MODEL

The quantum trajectories of noisy random circuits generally undergo monitored dynamics. When tuning the decoherence rate, the trajectory averaged entanglement entropy can undergo a measurement-induced transition from a volume- to an area-law scaling [1–3], indicating a critical decoherence rate p_c above which efficient classical simulation is possible. Our goal is to find an optimized unraveling scheme that yields the lowest p_c . In this section, we derive such an unraveling scheme for noisy random unitary circuits based on the effective spin model [4, 5]. Here, we consider unraveling every decoherence channel in the same basis. Moreover, we focus on the unraveling schemes with a minimum number of Kraus operators, which are related to the minimum set by a unitary transformation (see Sec. SI).

The central quantity of interest is the trajectory averaged von Neumann entropy for subsystem A

$$S_A = \mathbb{E}_U \left[- \sum_m p_m \text{tr}(\rho_{A,m} \log \rho_{A,m}) \right], \quad (\text{S10})$$

where p_m is the probability for each quantum trajectory labeled by m , and $\mathbb{E}_U[\cdot]$ represents averaging over random circuit realizations. However, analytically evaluating such a quantity is challenging. Instead, one can consider a series of quasi-entropy that approximates the true von Neumann entropy

$$\tilde{S}_A^{(n)} = \frac{1}{1-n} \log \left(\frac{\mathbb{E}_U[\sum_m p_m^n \operatorname{tr} \rho_{A,m}^n]}{\mathbb{E}_U[\sum_m p_m^n]} \right). \quad (\text{S11})$$

The quasi-entropies recover the von Neumann entropy in the replica limit $n \rightarrow 1$, i.e.

$$S_A = \lim_{n \rightarrow 1} \tilde{S}_A^{(n)}. \quad (\text{S12})$$

These quasi-entropies admit an analytic understanding in terms of the excess free energy of domain walls in effective spin models [4, 5]. These spin models undergo ferromagnetic transitions when tuning the decoherence rate, which manifest as the entanglement transition in the corresponding quasi-entropy. Thus, by minimizing the critical decoherence rate associated with the ferromagnetic transition in the spin model, one can obtain an optimized unraveling basis.

In this work, we focus on the second quasi-entropy $n = 2$. Although, the critical point $p_c^{(2)}$ associated with the second quasi-entropy only approximate p_c , the optimized unraveling scheme still significantly reduces the von Neumann entropy in trajectories as demonstrated by numerics in Sec. SV. Remarkably, the corresponding spin model for $n = 2$ is exactly solvable, allowing us to analytically determine the unraveling scheme that gives the lowest critical decoherence rate.

Following the derivation in Ref. [4], the effective spin model for $n = 2$ is a two-dimensional classical Ising model on a triangular lattice as shown in Fig. 2(a) in the main text. The model involves ferromagnetic J_d and anti-ferromagnetic Ising coupling J_h on the diagonal and horizontal bonds, respectively,

$$J_d = \frac{1}{4} \log \left(\frac{-u_2^2/q^2 + u_1^2}{u_2^2 - u_1^2/q^2} \right), \quad J_h = \frac{1}{4} \log \left\{ \frac{[u_1 u_2 (1 - 1/q^2)]^2}{(u_2^2 - u_1^2/q^2)(u_1^2 - u_2^2/q^2)} \right\}, \quad (\text{S13})$$

where q is the local Hilbert space dimension, and u_1 and u_2 are determined by the Kraus operators,

$$u_1 = \sum_{\alpha=0}^{N-1} (\operatorname{tr} K_{\alpha}^{\dagger} K_{\alpha} K_{\alpha}^{\dagger} K_{\alpha}), \quad u_2 = \sum_{\alpha=0}^{N-1} (\operatorname{tr} K_{\alpha}^{\dagger} K_{\alpha})^2. \quad (\text{S14})$$

We note that $\{K_{\alpha}\}$, also both u_1 and u_2 are functions of p .

The triangular lattice Ising model is exactly solvable [6, 7], and the critical point $p_c^{(2)}$ can be determined from

$$2e^{2J_h} = e^{-2J_d} - e^{2J_d}, \quad (\text{S15})$$

which is equivalent to

$$\left(\frac{u_2}{u_1} \right)^2 - 2 \frac{q^2 - 1}{q^2 + 1} \left(\frac{u_2}{u_1} \right) - 1 = 0, \quad (\text{S16})$$

For qubit system ($q = 2$), the solution of Eq. (S16) reads

$$\frac{u_2}{u_1} = \frac{1}{5} (3 + \sqrt{34}). \quad (\text{S17})$$

One can then solve for the critical point $p_c^{(2)}$ given u_1 and u_2 as functions of p .

The Kraus operators for different unraveling schemes are related by

$$K'_{\alpha} = \sum_{\beta=1}^{N-1} U_{\alpha\beta} K_{\beta}. \quad (\text{S18})$$

While U can be an isometry in general, we focus on decomposing the quantum channel in terms of a minimum number of Kraus operators and U being a unitary rotation in this work. Our goal is to find the unitary transformation that gives the minimum $p_c^{(2)}$. In general, it can be hard to solve for an analytical expression of U that gives the minimum $p_c^{(2)}$; however, a numerical optimization algorithm is always possible, as long as the search space is small. For a qubit system, any local quantum channel can be represented with at most four Kraus operators. Therefore, we can always parameterize U as using at most 15 parameters (SU(4) group has 15 free parameters) and perform numerical optimization. The spin-model optimized $p_c^{(2)}$ for dephasing, amplitude damping, and depolarization channels are summarized in Table S1.

For dephasing and amplitude damping channels, the unraveling scheme that gives the minimum $p_c^{(2)}$ can be analytically determined. Below, we derive the minimum $p_c^{(2)}$ and the associated Kraus operators for these two channels.

Unraveling basis	Conventional	Optimized
Dephasing	0.3558	0.0685
Depolarization	0.4386	0.0457
Amplitude damping	0.4205	0.1324

TABLE S1. Critical decoherence rate $p_c^{(2)}$ in the effective spin model for noisy random circuits. $p_c^{(2)}$ in the conventional and optimized unraveling scheme for dephasing, depolarization, and amplitude damping channel are presented.

1. Dephasing channel

For the dephasing channel, we consider the Kraus operators related to the minimum set [Eq. (S4)] by a general SU(2) unitary transformation

$$\begin{pmatrix} K_0 \\ K_1 \end{pmatrix} = \begin{pmatrix} e^{i(\psi+\phi)} \cos \theta & ie^{i(\psi-\phi)} \sin \theta \\ ie^{-i(\psi-\phi)} \sin \theta & e^{-i(\psi+\phi)} \cos \theta \end{pmatrix} \begin{pmatrix} \sqrt{1-\frac{p}{2}} \mathbb{1} \\ \sqrt{\frac{p}{2}} Z \end{pmatrix}. \quad (\text{S19})$$

Using this parameterization, the couplings are given by

$$u_1 = 2 \left\{ \left[\left(1 - \frac{p}{2} \right)^2 + \left(\frac{p}{2} \right)^2 \right] (\cos^4 \theta + \sin^4 \theta) + 4 \left(1 - \frac{p}{2} \right) \left(\frac{p}{2} \right) \cos^2 \theta \sin^2 \theta (2 + \sin^2 2\phi) \right\}, \quad (\text{S20})$$

$$u_2 = 4 \left\{ \left[\left(1 - \frac{p}{2} \right)^2 + \left(\frac{p}{2} \right)^2 \right] (\cos^4 \theta + \sin^4 \theta) + 4 \left(1 - \frac{p}{2} \right) \left(\frac{p}{2} \right) \cos^2 \theta \sin^2 \theta \right\}, \quad (\text{S21})$$

which has no dependency on ψ . Since u_2/u_1 is a non-increasing function of both p and $\sin^2 2\phi$, there is a tradeoff between $p_c^{(2)}$ and $\sin^2 2\phi$ at the critical point [Eq. (S17)]. Therefore, the minimum $p_c^{(2)}$ must be found when $\sin^2 2\phi$ is maximized ($\phi = \pi/4$ and $\sin^2 2\phi = 1$).

Then, one can search along θ to find the optimal $p_c^{(2)} = 0.0685$ at $\theta = \pi/4$. Choosing $\psi = -\pi/4$ (real-valued unitary transformation), the resulting Kraus operators are

$$\begin{pmatrix} K_0 \\ K_1 \end{pmatrix} = \frac{1}{\sqrt{2}} \begin{pmatrix} 1 & 1 \\ -1 & 1 \end{pmatrix} \begin{pmatrix} \sqrt{1-\frac{p}{2}} \mathbb{1} \\ \sqrt{\frac{p}{2}} Z \end{pmatrix}. \quad (\text{S22})$$

2. Amplitude damping channel

The Kraus operator for the amplitude damping channel can be derived analogously. We consider a SU(2) unitary transformation of the conventional unraveling [Eq. (S6)] as

$$\begin{pmatrix} K_0 \\ K_1 \end{pmatrix} = \begin{pmatrix} e^{i(\psi+\phi)} \cos \theta & ie^{i(\psi-\phi)} \sin \theta \\ ie^{-i(\psi-\phi)} \sin \theta & e^{-i(\psi+\phi)} \cos \theta \end{pmatrix} \begin{pmatrix} |0\rangle\langle 0| + \sqrt{1-p} |1\rangle\langle 1| \\ \sqrt{p} |0\rangle\langle 1| \end{pmatrix}. \quad (\text{S23})$$

This gives rise to

$$u_1 = 2(1 - p + p^2) (\cos^4 \theta + \sin^4 \theta) + 4p(2 - p) \cos^2 \theta \sin^2 \theta, \quad (\text{S24})$$

$$u_2 = 2(2 - 2p + p^2) (\cos^4 \theta + \sin^4 \theta) + 4p(2 - p) \cos^2 \theta \sin^2 \theta. \quad (\text{S25})$$

Here, u_1 and u_2 are only functions of θ , where the unraveling that minimizes $p_c^{(2)}$ can be found at $p_c^{(2)} = 0.1324$ compared to the conventional unraveling with $p_c^{(2)} = 0.4205$. Choosing $\psi = -\pi/4$ and $\phi = \pi/4$ (real-valued unitary transformation), the resulting Kraus operators are

$$\begin{pmatrix} K_0 \\ K_1 \end{pmatrix} = \frac{1}{\sqrt{2}} \begin{pmatrix} 1 & 1 \\ -1 & 1 \end{pmatrix} \begin{pmatrix} |0\rangle\langle 0| + \sqrt{1-p} |1\rangle\langle 1| \\ \sqrt{p} |0\rangle\langle 1| \end{pmatrix}. \quad (\text{S26})$$

SIII. DETAILS FOR HEURISTIC OPTIMIZATION ALGORITHM

For the heuristic optimization method, we minimize the average entropy of the noisy system qubit averaged over the measurement outcomes of the ancilla qudit. We note that since the entropy of the noisy qubit is state-dependent, the optimized unraveling depends on previous measurement outcomes. In this sense, the optimized unraveling scheme in the heuristic algorithm is, strictly speaking, achieved by a nonlocal unitary transformation on ancilla qudits, which involves local operations and classical communication. In other words, this algorithm is adaptive. Moreover, although decoherence channels at the same time step commute with each other, the order in which their unraveling basis is optimized could potentially affect the resulting state in trajectories. In this work, we choose the order of the optimization sequentially from qubit 1 to qubit L for dephasing channels within a single time step.

SIV. TROTTERIZATION OF LINDBLAD EQUATION

For a generic Lindblad equation

$$\dot{\rho} = -i[H, \rho] + \sum_i \gamma_i \left(L_i \rho L_i^\dagger - \frac{1}{2} \{ L_i^\dagger L_i, \rho \} \right), \quad (\text{S27})$$

we can trotterize the unitary evolution with respect to H and the quantum jumps with respect to $\{L_i\}$, as

$$\rho(t + dt) = \mathcal{N}_{dt} [e^{-iHdt} \rho(t) e^{iHdt}] + \mathcal{O}(dt^2), \quad (\text{S28})$$

where the decoherence channel \mathcal{N}_{dt} is further decomposed into product of local channels, i.e. $\mathcal{N}_{dt} = \prod_i \mathcal{N}_{i,dt}$. Each local channel only involves the jump operators L_i that apply on a single qubit and is described by the following Kraus operators

$$K_0 = \mathbb{1} - \frac{dt}{2} \sum_i \gamma_i L_i^\dagger L_i, \quad K_{\alpha > 0} = \sqrt{\gamma_\alpha dt} L_\alpha. \quad (\text{S29})$$

The Hamiltonian evolution operator e^{-iHdt} is also trotterized to achieve the brick-layer structure as used in this work.

For dephasing error where $L_i = Z_i$ and $\gamma_i = \gamma$, we arrive at

$$K_0 = \left(1 - \frac{dt}{2} \gamma \right) \mathbb{1}, \quad K_1 = \sqrt{\gamma dt} Z_i, \quad (\text{S30})$$

which agrees with the unital unraveling of the dephasing channel with $p = 2\gamma dt$ up to the lowest order in dt .

SV. ADDITIONAL NUMERICAL RESULTS

In this section, we provide additional numerical results for the critical decoherence rates associated with the von Neumann entropy and Renyi entropies in three different unravelings of the dephasing channel. The extracted critical decoherence rate p_c for RUC and MFIM are presented in Table S2 and S3, respectively. The tripartite mutual information as a function of decoherence rate p and the finite-size scaling analysis used to determine p_c can be found in Fig. S1-S6

Unraveling basis	Conventional	Spin-model Optimized	Heuristically Optimized
Renyi-1/2	0.196(3)	0.097(3)	0.096(3)
Von Neumann	0.168(3)	0.089(3)	0.085(2)
Renyi-2	0.165(4)	0.102(3)	0.102(3)
Renyi- ∞	0.172(5)	0.110(4)	0.110(3)

TABLE S2. Critical decoherence rate p_c for RUC with dephasing noise for various Renyi indices extracted from finite size scaling collapse.

Unraveling basis	Conventional	Spin-model Optimized	Heuristically Optimized
Renyi-1/2	0.222(5)	0.121(7)	0.116(8)
Von Neumann	0.201(6)	0.111(6)	0.100(6)
Renyi-2	0.196(7)	0.126(6)	0.119(9)
Renyi- ∞	0.205(8)	0.135(8)	0.124(8)

TABLE S3. Critical decoherence rate γ_c for MFIM with dephasing noise for various Renyi indices extracted from finite size scaling collapse.

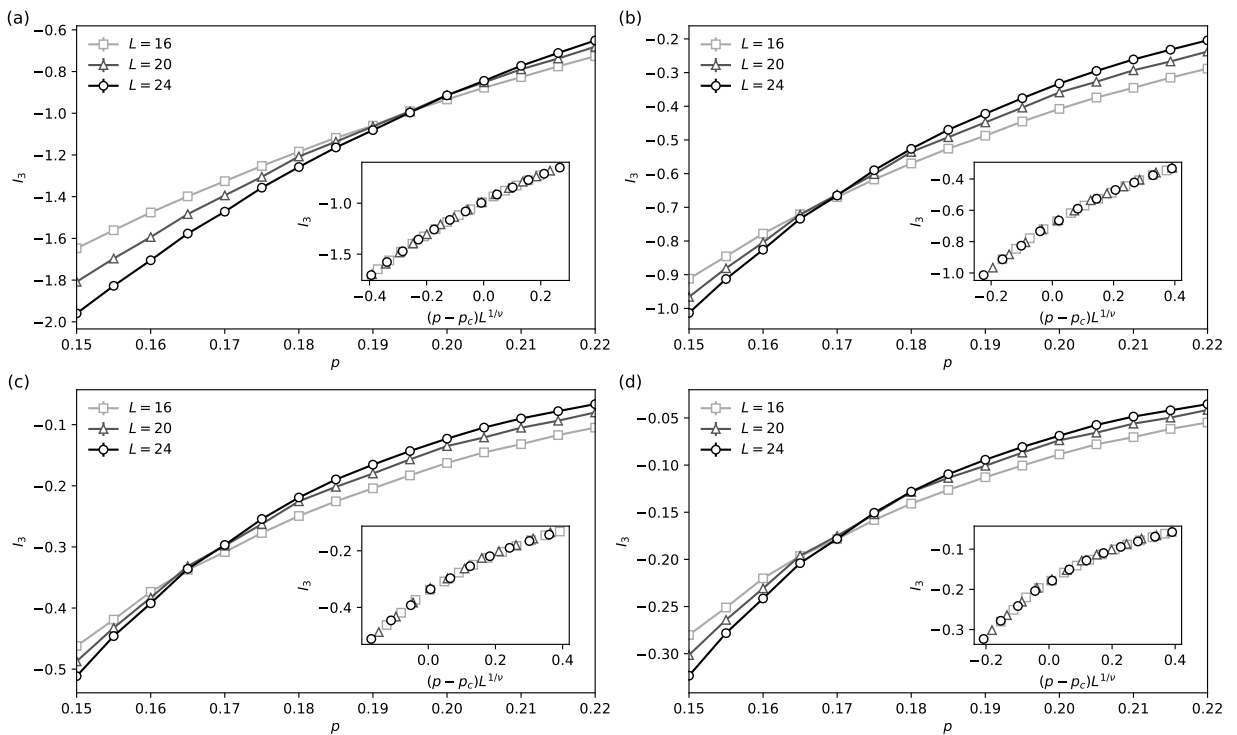


FIG. S1. Tripartite mutual information I_3 as a function of the decoherence rate p in the computational unravelling basis for RUC. (Inset) Finite-size scaling collapse to determine the critical decoherence rate. Subplots: (a) Renyi-1/2 entropy; (b) von Neumann entropy; (c) Renyi-2 entropy; and (d) Renyi- ∞ entropy. The results are averaged over 400 quantum trajectories. The results here are consistent with Ref. [8].

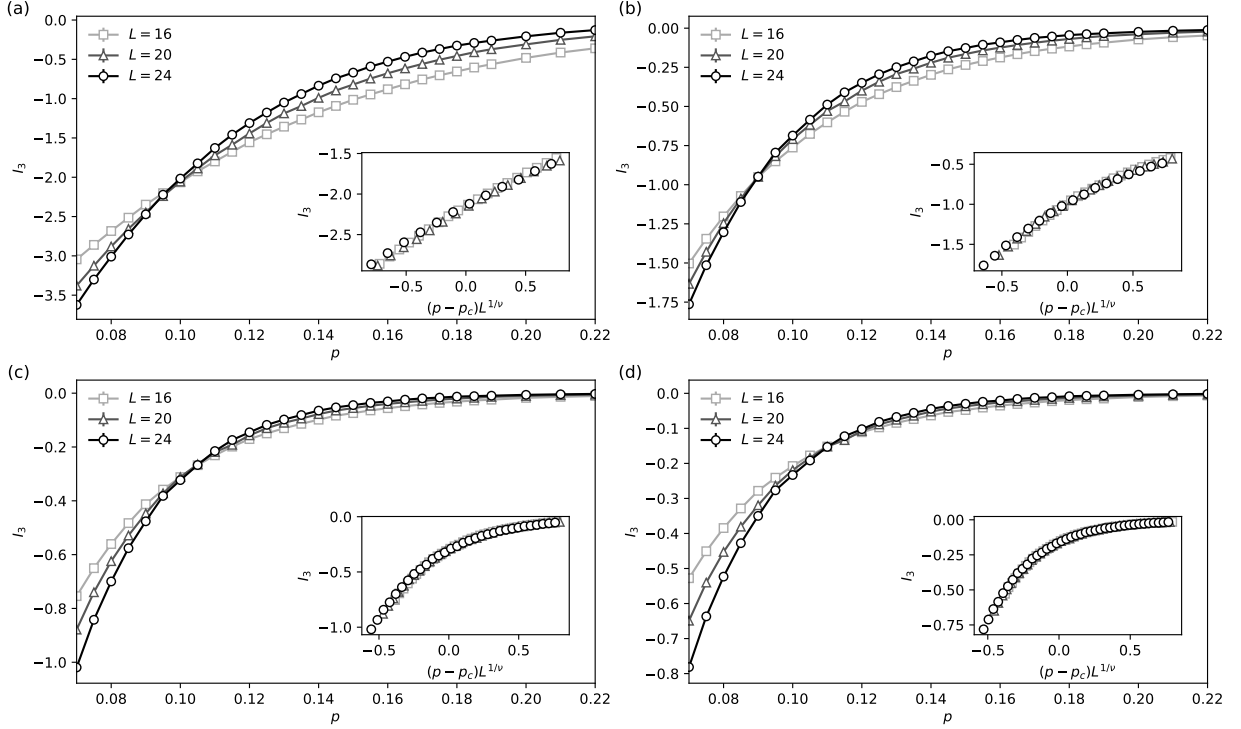


FIG. S2. Tripartite mutual information I_3 as a function of the decoherence rate p in the spin-model optimized unraveling basis for RUC. (Inset) Finite-size scaling collapse to determine the critical decoherence rate. Subplots: (a) Renyi-1/2 entropy; (b) von Neumann entropy; (c) Renyi-2 entropy; and (d) Renyi- ∞ entropy. The results are averaged over 400 quantum trajectories.

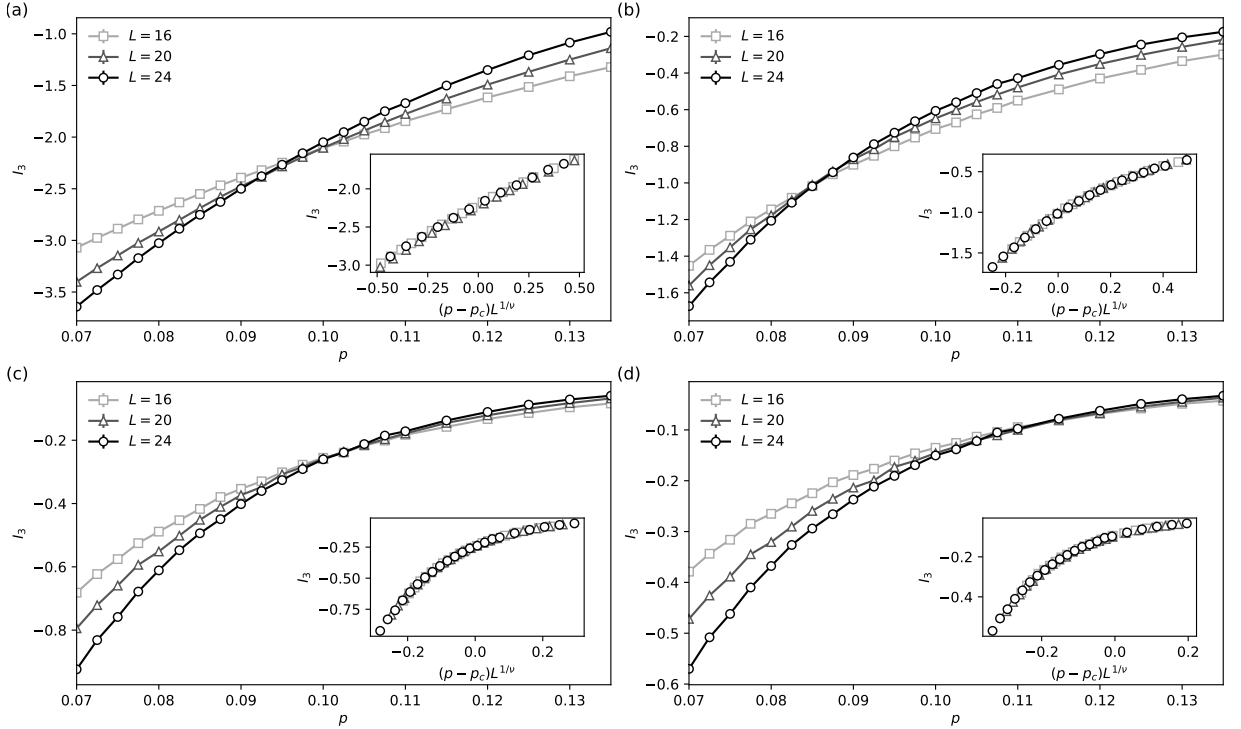


FIG. S3. Tripartite mutual information I_3 as a function of the decoherence rate p in the heuristically optimized unraveling basis for RUC. (Inset) Finite-size scaling collapse to determine the critical decoherence rate. Subplots: (a) Renyi-1/2 entropy; (b) von Neumann entropy; (c) Renyi-2 entropy; and (d) Renyi- ∞ entropy. The results are averaged over 400 quantum trajectories.

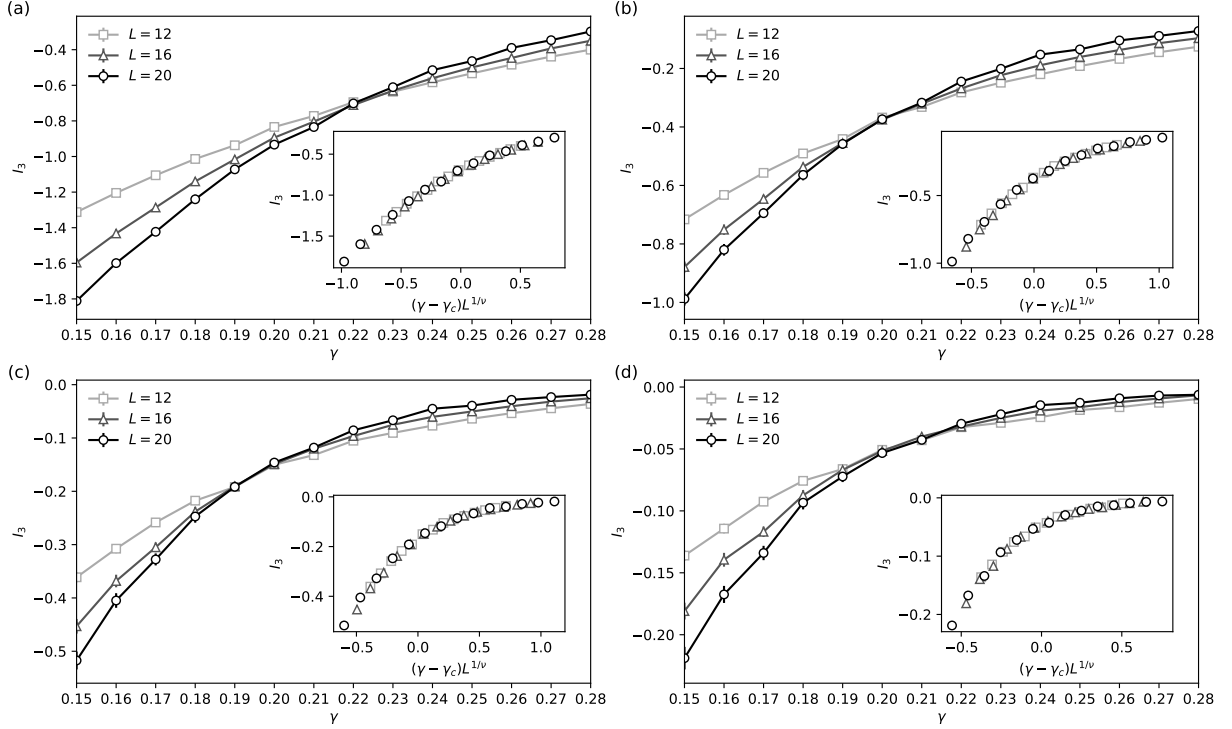


FIG. S4. Tripartite mutual information I_3 as a function of the decoherence rate γ in the computational unravelling basis for MFIM. (Inset) Finite-size scaling collapse to determine the critical decoherence rate. Subplots: (a) Renyi-1/2 entropy; (b) von Neumann entropy; (c) Renyi-2 entropy; and (d) Renyi- ∞ entropy. The results are averaged over 100 quantum trajectories.

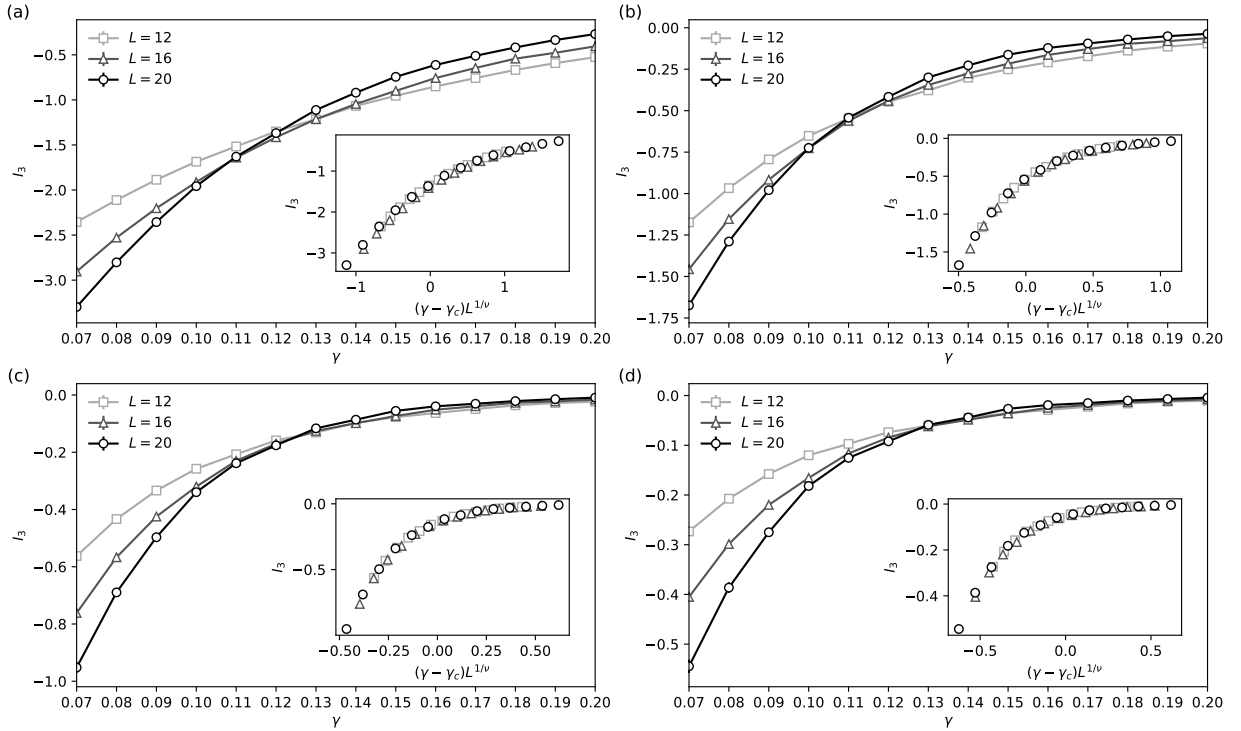


FIG. S5. Tripartite mutual information I_3 as a function of the decoherence rate γ in the spin-model optimized unravelling basis for MFIM. (Inset) Finite-size scaling collapse to determine the critical decoherence rate. Subplots: (a) Renyi-1/2 entropy; (b) von Neumann entropy; (c) Renyi-2 entropy; and (d) Renyi- ∞ entropy. The results are averaged over 100 quantum trajectories.

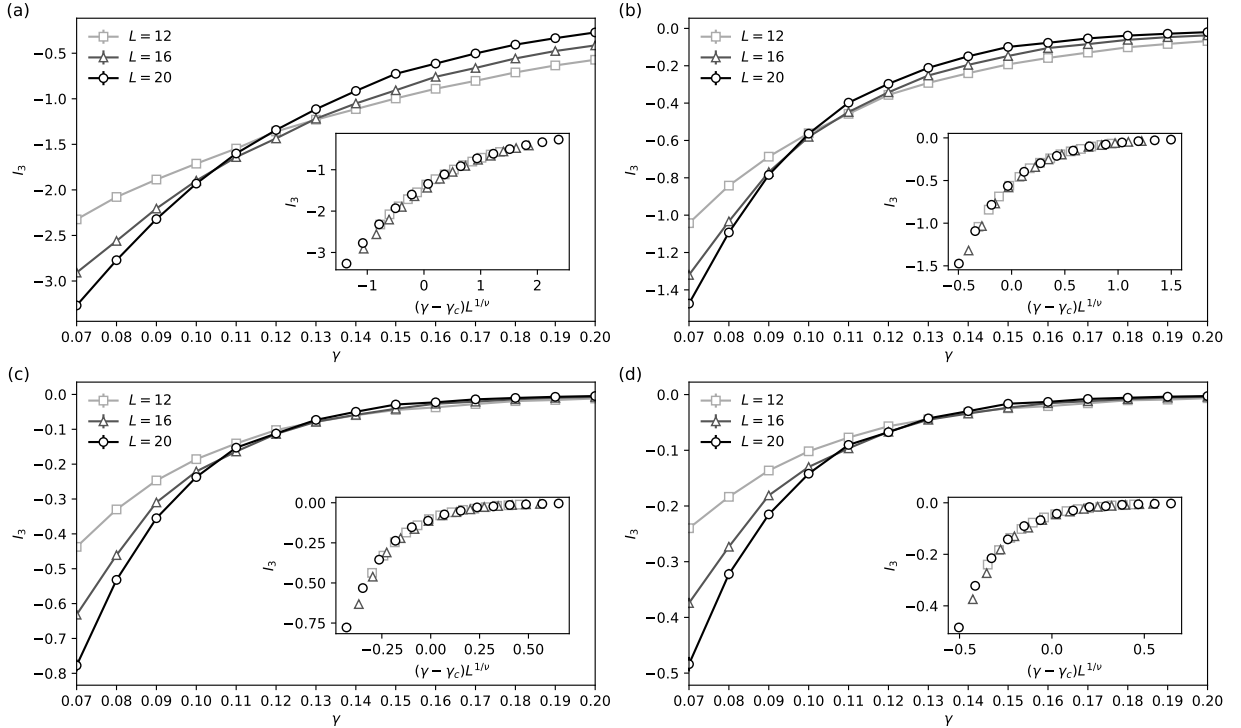


FIG. S6. Tripartite mutual information I_3 as a function of the decoherence rate γ in the heuristically optimized unraveling basis for MFIM. (Inset) Finite-size scaling collapse to determine the critical decoherence rate. Subplots: (a) Renyi-1/2 entropy; (b) von Neumann entropy; (c) Renyi-2 entropy; and (d) Renyi- ∞ entropy. The results are averaged over 100 quantum trajectories.

[1] Y. Li, X. Chen, and M. P. Fisher, Quantum zeno effect and the many-body entanglement transition, *Physical Review B* **98**, 205136 (2018).

[2] B. Skinner, J. Ruhman, and A. Nahum, Measurement-induced phase transitions in the dynamics of entanglement, *Physical Review X* **9**, 031009 (2019).

[3] Y. Li, X. Chen, and M. P. Fisher, Measurement-driven entanglement transition in hybrid quantum circuits, *Physical Review B* **100**, 134306 (2019).

[4] Y. Bao, S. Choi, and E. Altman, Theory of the phase transition in random unitary circuits with measurements, *Physical Review B* **101**, 104301 (2020).

[5] C.-M. Jian, Y.-Z. You, R. Vasseur, and A. W. Ludwig, Measurement-induced criticality in random quantum circuits, *Physical Review B* **101**, 104302 (2020).

[6] T. Eggarter, Triangular antiferromagnetic ising model, *Physical Review B* **12**, 1933 (1975).

[7] Y. Tanaka and N. Uryû, Triangular ising lattice with anisotropic interactions, *Journal of the Physical Society of Japan* **44**, 1091 (1978).

[8] A. Zabalo, M. J. Gullans, J. H. Wilson, S. Gopalakrishnan, D. A. Huse, and J. Pixley, Critical properties of the measurement-induced transition in random quantum circuits, *Physical Review B* **101**, 060301 (2020).